Spatial Distribution of Climatic Cycles in Andalusia (Southern Spain)

J. Sánchez-Morales, E. Pardo-Igúzquiza and F. J. Rodríguez-Tovar

Abstract Several climatic cycles in Andalusia (southern Spain) have been identified by using precipitation and temperature data from most of the twentieth and the early twenty-first centuries at 707 meteorological stations. Some of the cycles detected had been recognized in previous studies, such as the 3-year cycle and the 7/8-year cycle, which were the most common periodicities across the study area. Spectral analysis was used for statistical analysis. The power spectrum estimator used is the smoothed Lomb–Scargle periodogram. The results reveal very interesting spatial patterns that had not been seen before in previous climatic studies, which illustrate a combined and complex influence of the North Atlantic Oscillation and the Mediterranean Oscillation. In general, the precipitation record studied presents better results than the temperature record, which offers less clarity in assessing climatic variability in Andalusia. Nevertheless, most of the cycles identified in the precipitation record were detected in the temperature record as well.

Keywords Power spectrum · Climate · North Atlantic Oscillation · Mediterranean Oscillation · Andalusia · Spain

J. Sánchez-Morales (✉) · F. J. Rodríguez-Tovar
Universidad de Granada, Avd. Fuentenueva s/n, 18071 Granada, Spain
e-mail: josesanmor@correo.ugr.es; jose.chez.morales@gmail.com

F. J. Rodríguez-Tovar
e-mail: fjrtovar@ugr.es

E. Pardo-Igúzquiza
Instituto Geológico y Minero de España, Ríos Rosas 23, 28003 Madrid, Spain
e-mail: e.pardo@igme.es

Introduction

Andalusia (southern Spain) is a region characterized by huge climatic contrasts, i.e. the 'Sierra de Grazalema' in the southwest is the wettest place on the entire Iberian Peninsula with average rainfall of over 2000 mm/year, whereas the 'Desierto de Tabernas' in the southeast is considered the driest place in Continental Europe with less than 150 mm/year on average. The influence of both the Atlantic Ocean and the Mediterranean Sea on this area of 87,597 km^2, plus the presence of the Betic Cordillera with altitudes above 3000 m.s.l. (metres above sea level), make this region unique from a climatic point of view and very interesting for analysing the evolution of climate from past to present times, especially during the most recent periods. Thus, Andalusia could be seen as a natural laboratory for the study of climatic changes from past to present.

Climatic studies from the region of Andalusia are frequent and focus on a variety of aspects. Thus, several statistical techniques and methodologies have been used, i.e. principal component analysis [1], empirical orthogonal function [2], innovative missing values estimator [3], non-instrumental climate reconstruction [4], and gridded dataset and combined indices evolution [5], amongst many others.

The causes of climate variability in Andalusia at annual, inter-annual, decadal and multi-decadal timescales are generally associated with diverse phenomena, involving several climatic subsystems, revealing the interactions between the atmosphere and ocean [1–5]. In some cases, a cyclic pattern in climatic variability has been interpreted. The identification of climatic cycles in Andalusia by means of spectral analysis has been carried out in previous studies although the method differed according to the specific study [6, 7]. On this basis, this study examines climatic evolution during the twentieth and twenty-first centuries in Andalusia, based on the spectral analysis of data from different climatic proxies, in order to evaluate the cyclic nature of the said evolution and to interpret the processes involved.

Methodology

This study uses spectral analysis as a statistical technique to evaluate the importance of the frequencies associated with precipitation and temperature time series in Andalusia (see meteorological datasets below). The power spectrum estimator used is the smoothed Lomb–Scargle periodogram [8–10], which works directly with uneven time series, such as the annual precipitation and/or annual temperature series in the study area. The technique evaluates the statistical significance of the peaks using the Monte Carlo permutation test, as neighbouring frequencies are highly correlated, and then it adjusts statistical significance by smoothing the periodogram [10]. Linear smoothing with three terms was applied to the raw periodogram. The output consists of the Lomb–Scargle spectrum, the achieved confidence level spectrum, the mean spectrum of permutations and the phase spectrum.
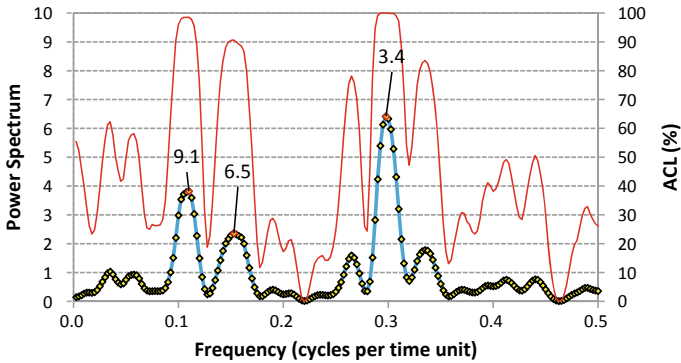
Fig. 1 Example of the power spectrum for annual precipitation at station P6289, and associated peaks of 9.1, 6.5 and 3.4 years above Achieved Confidence Level (ACL) of 90%, by using the smoothed Lomb–Scargle periodogram

The parameters required have been optimized for dealing with the annual precipitation and/or temperature time series in the study area, and for achieving the intended goal of capturing climatic cycles with a duration just above the sampling interval (i.e. biannual oscillation). Thus, 0.5 has been used as the highest frequency to evaluate, 200 as the number of frequencies in the interval, 2000 as the number of permutations, 75,654 as the random seed, 3 as the number of smoothing terms and linear smoothing was enabled. To illustrate the above process, the output of this methodology from one of the precipitation stations is presented below (Fig. 1).

Meteorological Datasets

The precipitation and temperature data were collected from two different sources and named chguadalquivir [11] and aemet [12]. The sources differ from each other with regard to the sampling interval; datasets from chguadalquivir were available monthly and covered the period from 1951 to 1987, whereas datasets from aemet were available daily and covered the period from 1901 to 2012. There were 1574 precipitation station and 526 temperature station datasets from chguadalquivir, spread across the entire study area. There were 595 precipitation station and 282 temperature station datasets from aemet, all located in the eastern half of the study area.

For a better comparison, all the datasets have been converted into annual datasets. As a first step, the daily datasets were summarized into monthly datasets; only months with a minimum of 25 days of precipitation measurements and/or a minimum of 20 days of temperature measurements were considered. Then, to convert the monthly datasets into annual datasets, only complete years and/or years that had 12 months of measurements were used. A second level of filtering was also carried out in which precipitation stations with less than a total of 20 years of records and temperature
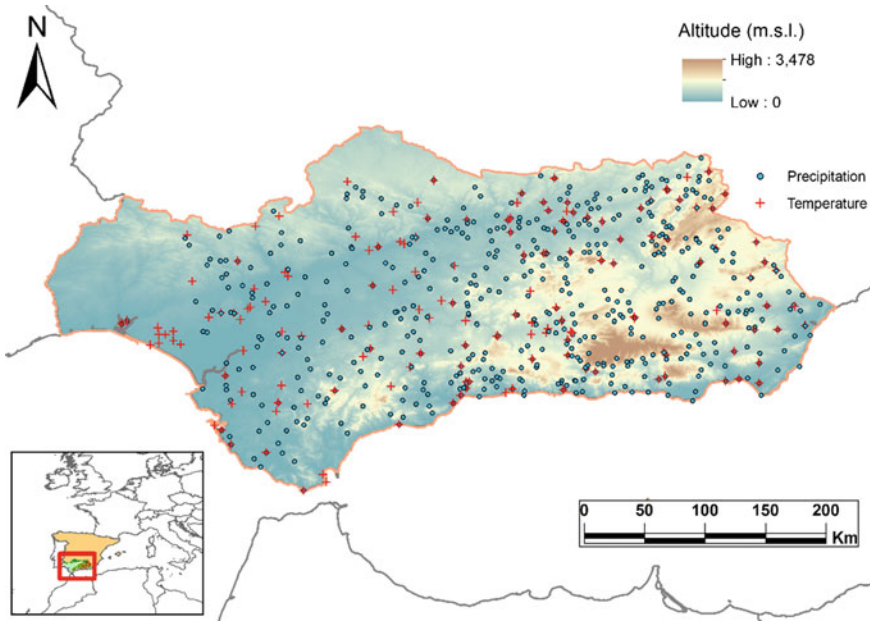
Fig. 2 Distribution of the meteorological stations selected for the spectral analysis

stations with less than a total 10 years of records were excluded from the analysis. It was not a requirement for that the total amount of years with records to be consecutive, as this spectral analysis methodology can deal with uneven series. Upon combining the two data sources, a comparison method was established to see which one had more years of information for the same station, as various stations were in both data sources. If the length of the series in years was the same in both sources, preference was given to the dataset from aemet, which was originally compiled daily.

The filtering process produced 547 precipitation stations and 160 temperature stations: a total of 707 meteorological datasets to be analysed (Fig. 2).

Results

The spectral analysis carried out on the 707 datasets detected 1751 significant peaks in the precipitation datasets (Fig. 3) and 466 significant peaks in the temperature datasets (Fig. 4), all above or equal to 90% of ACL. All the cycles detected for the same meteorological variable have been plotted in the same diagram.

The number of cycles detected is lower in the temperature record than in the precipitation record, but it is very remarkable that both temperature and precipitation variables show signals at the same frequencies. The 3-year cycle and the 7/8-year
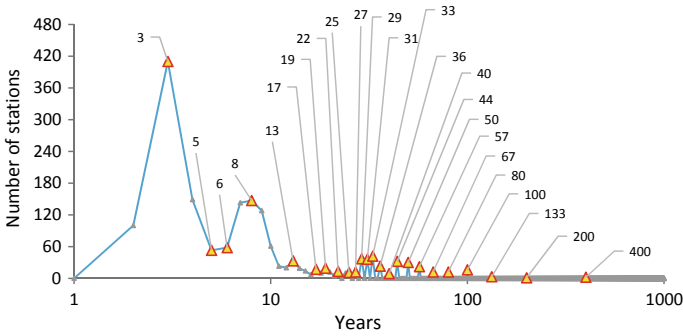
Fig. 3 Diagram containing all the precipitation cycles in the study area and the number of stations in which the cycles were detected (yellow triangles represent the value of the cycle in years)
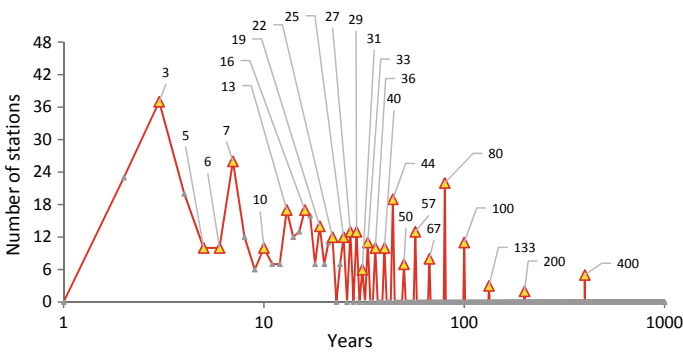

Fig. 4 Diagram containing all the temperature cycles in the study area and the number of stations in which the cycles were detected (yellow triangles represent the value of the cycle in years)

cycle were the most frequently detected, and show the highest significance. Thus, a detailed analysis of cycles at both 3 years and 7/8 years has been conducted.

All precipitation (344) and temperature (28) stations showing peaks between frequency values of 0.4 (2.5 years) and 0.29 (3.5 years) have been collected and plotted on a map to see their spatial distribution (Fig. 5). The same output has been conducted for the 7/8-year cycle by isolating all peaks between 0.154 (6.5 years) and 0.118 (8.5 years), 223 precipitation stations and 23 temperature stations (Fig. 6).

Overall (Figs. 5 and 6), the spatial distribution of temperature observed does not show any geographical predominance of one cycle over the other, as opposed to the maps showing the precipitation cycles observed, where a general trend can be inferred. In the latter, there are more 3-year cycles in the east and more 7/8-year cycles in the west. The two cycles have been combined into one map by using all the precipitation stations in which the two cycles were detected together (Fig. 7). This process was based on a preliminary selection of stations in which at least one of the two cycles must be present at each station; if both cycles were detected in the same
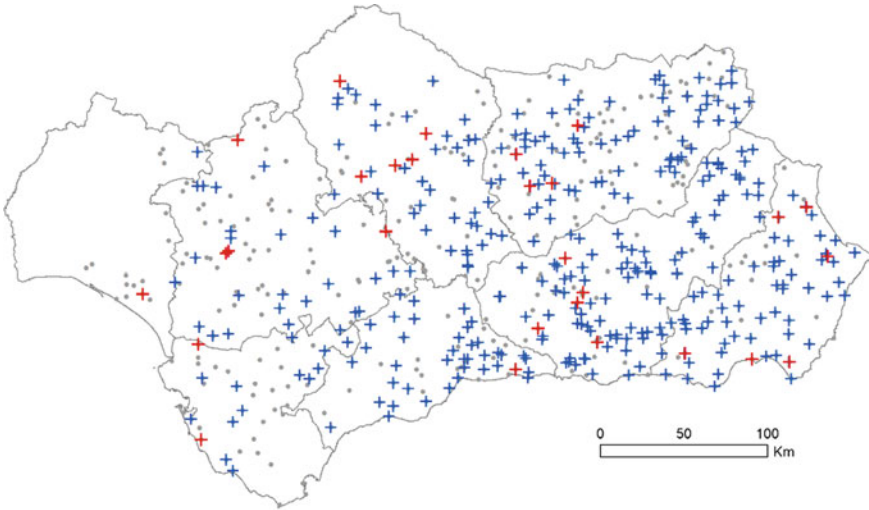
Fig. 5 Spatial distribution of all precipitation and temperature stations in which the 3-year cycle was detected (crosses in blue for precipitation and red for temperature) above 90% of ACL, and all the other stations used for the analysis (points in grey)
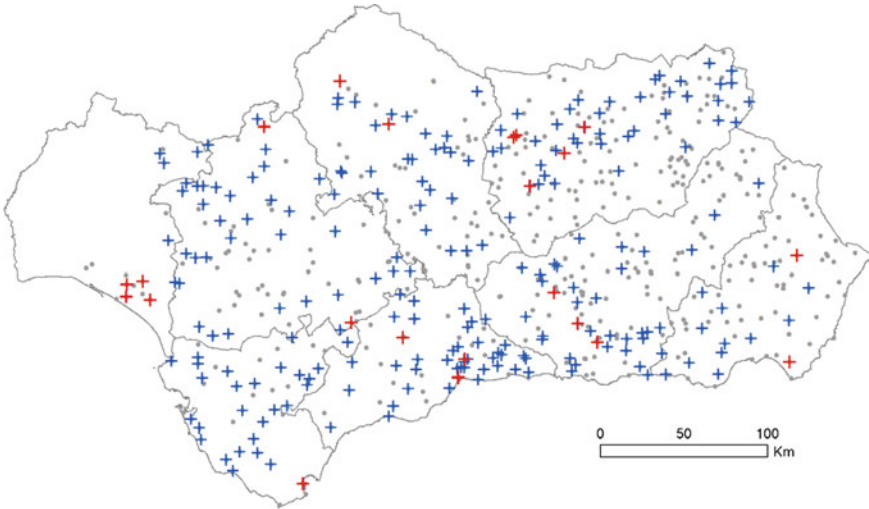

Fig. 6 Spatial distribution of all precipitation and temperature stations in which the 7/8-year cycle was detected (crosses in blue for precipitation and red for temperature) above 90% of ACL, and all the other stations used for the analysis (points in grey)
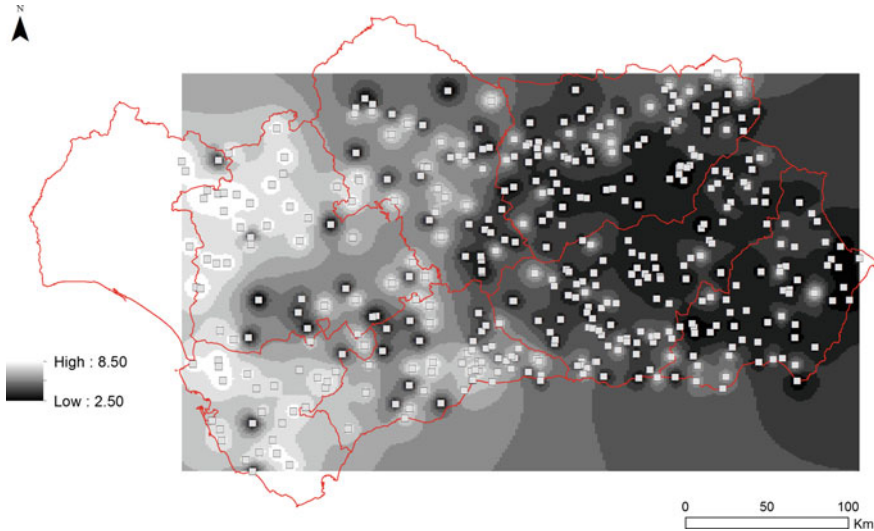
Fig. 7 Spatial interpolation on 423 precipitation stations showing the geographical influence in Andalusia on the 3-year cycle and the 7/8 year cycle. Values from 2.50 to 8.50 in years

station, the cycle with more power spectrum was the one counted for that station. Thus, 423 precipitation stations resulting from the aforementioned conditions have been analysed. About 261 precipitation stations show a predominance of the 3-year cycle and 162 precipitation stations show a predominance of the 7/8-year cycle. This process was followed by an interpolation process in which the 'Inverse Distance Weighting' technique was applied. The parameters were '2' for the power and '5' for the maximum number of neighbours.

Interpretation

The causes of climate variability in Andalusia from annual to multi-decadal timescales have generally been associated with Atlantic Ocean phenomena: large scale circulation features of Western Europe and the Atlantic Ocean [1], alternation of zonal circulation and meridional circulation in the Atlantic that shifts the Azores High [2], persistency and displacement of the Azores High [3], and changes in North Atlantic Oscillation (NAO) phases [4]. However, Eastern Andalusia is less influenced by Atlantic air masses and climate variability there is also influenced by Mediterranean Sea dynamics [5].

Previous studies applying spectral analysis to climatic datasets reveal cyclic climatic variability in the range of 2–250 years, but mainly located in the range of 2–11 years. Thus, a study on rainfall variability in Southern Spain [6] found peaks above 95% significance at 2.1, 3.5, 7–9, 16.7 and 250 years, and a previous study on

hydraulic heads across the Vega de Granada aquifer [7] found a decadal cycle (peaks
between 8 and 11 years) and a 3.2-year cycle, amongst others.

The power spectrum has been estimated for both North Atlantic Oscillation and
Mediterranean Oscillation indexes (MOI) (Figs. 8 and 9). The NAO index is available
at a daily resolution [14] from 1950 to 2017. The MOI has two versions [15], 'Algiers-
Cairo' (MOAC) and 'Israel-Gibraltar' (MOIG), both from 1948 to 2016 at daily
resolution. The NAO and MOIG indexes have been analysed by using annual series.

The NAO index has significant periodicities at 50, 13.7, 2.7, 2.5 and 2.1 years,
and the MOIG index at 7.8, 6.5, 4.1, 3.4, 2.4 and 2.1 years, all above 90% of ACL.

A second exercise has been conducted to assess the correlation between all the
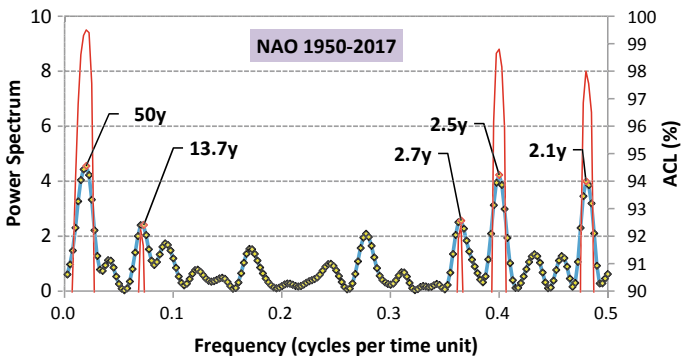monthly series from the 707 stations (547 precipitation stations and 160 tempera-

Fig. 8 Power spectrum of the NAO index using annual records derived from the original dataset,
and associated peaks of 50, 13.7, 2.7, 2.5 and 2.1 years above ACL of 90%, by using the smoothed
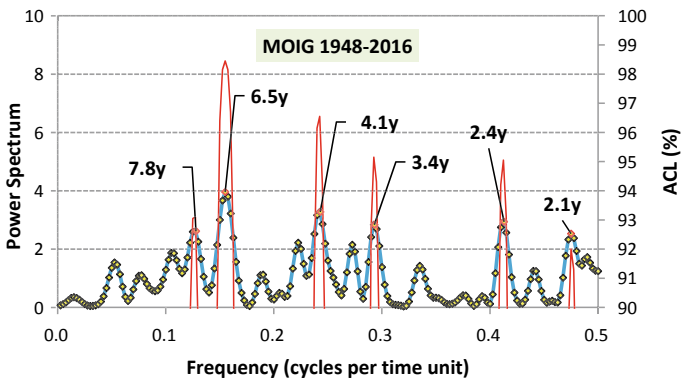Lomb–Scargle periodogram

Fig. 9 Power spectrum of the MOIG index using annual records derived from the original dataset,
and associated peaks of 7.8, 6.5, 4.1, 3.4, 2.4 and 2.1 years above ACL of 90%, by using the
smoothed Lomb–Scargle periodogram

ture stations) and the NAO and MO indexes. The geographical influence of both oscillations has been assessed (Figs. 10, 11, 12 and 13). The NAO correlation for precipitation (Fig. 10) is low; it tends to be more negative towards the west (−0.343) and zero or slightly positive towards the east (0.067). The NAO and temperature correlation (Fig. 11) is less clear, with values between −0.214 and 0.240. The MOIG and precipitation correlation (Fig. 12) is greater in value (from −0.16 to −0.76) than that of the NAO and is always negative; it shows a pattern of being more negative towards the west (−0.753) and less negative towards the east (−0.240). The correlation between MOIG and temperature (Fig. 13) is always positive, with values between 0.386 and 0.643, and it is equally distributed across the study area.

The most significant frequencies associated with both the NAO and MOIG indexes have been combined, as have the power spectra frequencies detected above 90% of ACL (Figs. 14 and 15). Certain precipitation and temperature frequency values match some of the frequencies associated with NAO and MOIG quite well.

Particularly interesting are the precipitation cycles that correspond to the MOIG cycles of 3.4, 6.5 and 7.8 years, and to the NAO cycles of 2.1, 2.7, 14.3 and 50 years. The match between the temperature cycles recorded and the NAO and MOIG cycles is less clear than the precipitation comparison.

Other cycles detected in the study area, which were also above 90% of ACL, could be tentatively associated with other climatic phenomena (Table 1; [13] for a review).
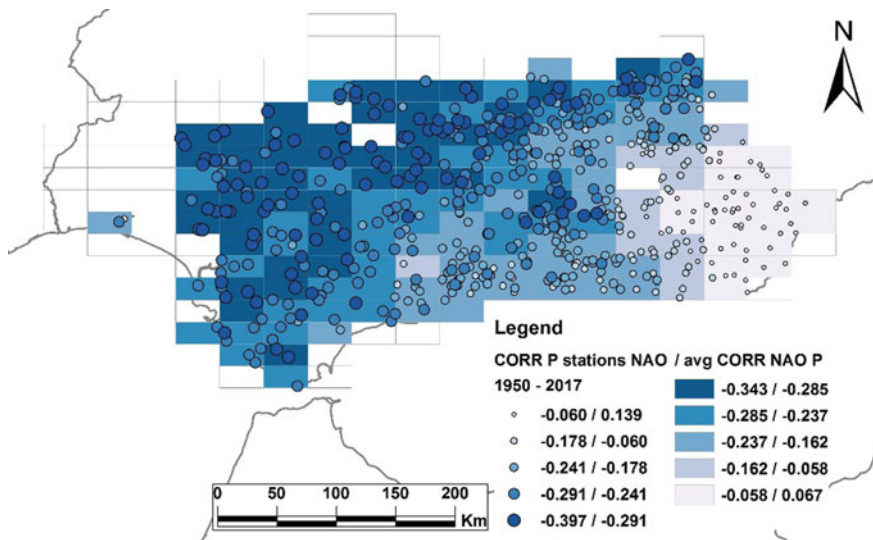

Fig. 10 Correlation coefficients between the NAO index monthly values (1950–2017) and the monthly values of the 547 precipitation stations. The rectangles represent the average value for that particular area
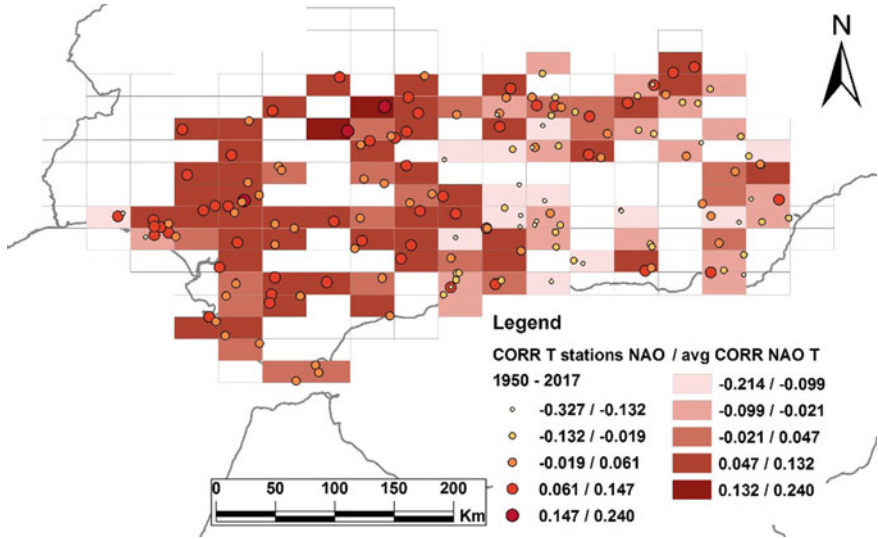
Fig. 11 Correlation coefficients between the NAO index monthly values (1950–2017) and the monthly values of the 160 temperature stations. The rectangles represent the average value for that particular area
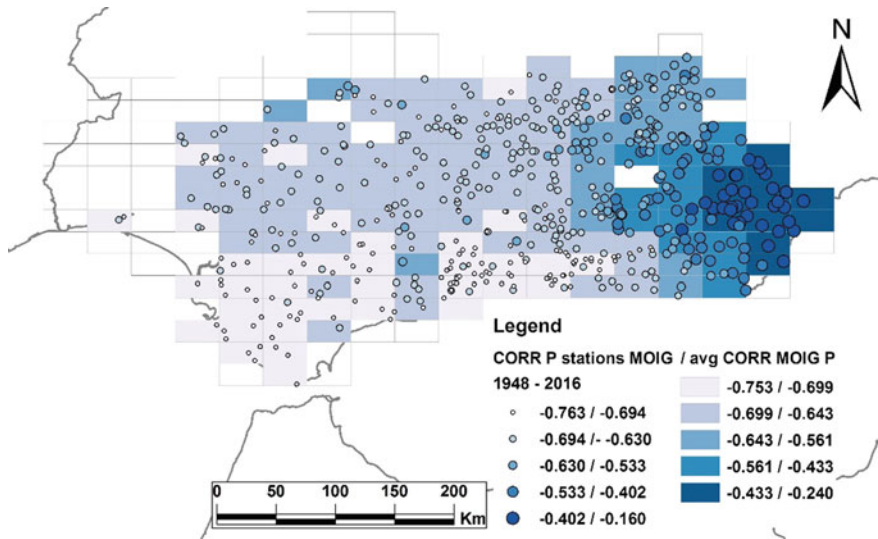

Fig. 12 Correlation coefficients between the MOIG index monthly values (1948–2016) and the monthly values of the 547 precipitation stations. The rectangles represent the average value for that particular area
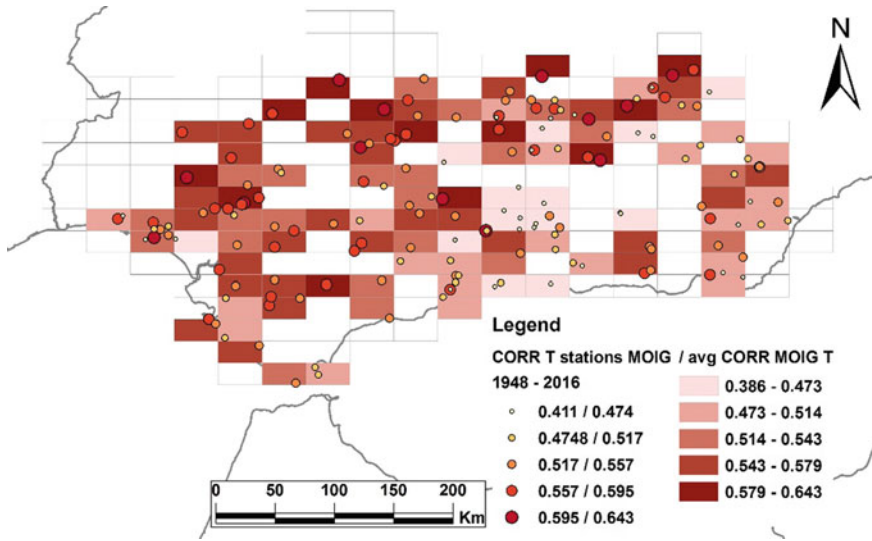
Fig. 13 Correlation coefficients between the MOIG index monthly values (1948–2016) and the monthly values of the 160 temperature stations. The rectangles represent the average value for that particular area
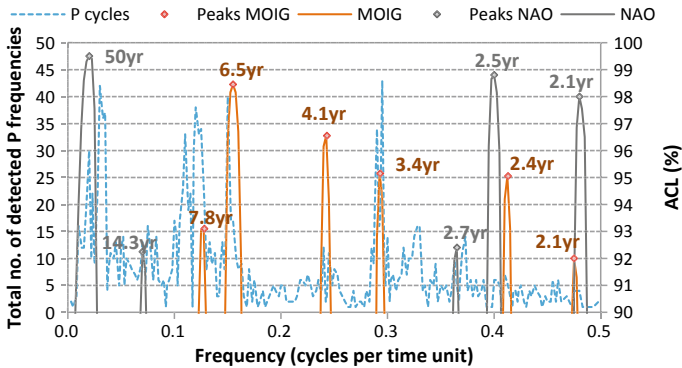

Fig. 14 Histogram of frequencies detected above ACL 90% from all precipitation stations, together with the most significant frequencies of the NAO and MOIG indexes

Conclusions

Spectral analysis of precipitation and temperature time series from a considerable number of meteorological stations (707 locations) distributed across southern Spain in the region of Andalusia has allowed for the characterization of the spatial variability of the two most frequent cycles in the study region: a 7/8-year cycle and a 3-year cycle. The length of time over which data was collected at the stations analysed was
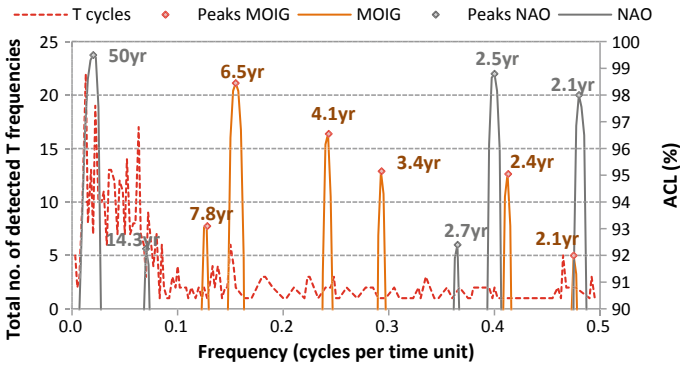
Fig. 15 Histogram of frequencies detected above ACL 90% from all temperature stations, together with the most significant frequencies of the NAO and MOIG indexes

Table 1 Tentative correlation between the other cycles detected above 90% ACL and other well known cycles, including the number of precipitation (P) and temperature (T) stations where the said cycles were detected

Cycle value in years	Cycle	P	T
10/11	Sunspot cycles of 11 years	84	17
17	Southern Oscillation Index (SOI)	17	16
19	Lunisolar cycle	19	14
20–25	Hale cycle	51	49

relatively short (in most cases less than 50 years, but always more than 20 years for precipitation and 10 years for temperature) and therefore the focus of this research has been the high-frequency cycles. Many other periodicities greater than 10 years have been found with an ACL higher than 90%, but they are less abundant. Initially, it was thought that the western part of the study area might be more influenced by the climatic activity derived from the North Atlantic Oscillation (NAO), manifesting as a cycle in the range from 7 to 8 years. On the other hand, the eastern part of the study area was hypothesized to be more influenced by the Mediterranean Oscillation (MO), represented by a 3-year cycle. However, the correlation values calculated across the study area between the meteorological variables on the one hand, and the NAO and MOIG indexes on the other, plus the spectral analysis conducted, show that the Mediterranean Oscillation may play a greater role in the region than the North Atlantic Oscillation. Thus, the 7/8-year cycle may correspond to the 6.5- and 7.8-year cycles detected in the MOIG index, and the 3-year cycle may be associated with the 3.4-year cycle detected in the MOIG index, and with the 2.7- and 2.5-year cycles detected in the NAO index. The explanation of how these two climatic phenomena interact with one another is outside the scope of this paper and more research is needed. Nevertheless, these results can help meteorologists and climatologists to better understand how weather and climate work in the southern Iberian Peninsula.

References

1. Esteban-Parra, M.J., Rodrigo, F.S., Castro-Díez, Y.: Spatial and temporal patterns of precipitation in Spain for the period 1880–1992. Int. J. Climatol. **18**(14), 1557–1574 (1998)
2. Rodrigo, F.S., Esteban-Parra, M.J., Pozo-Vázquez, D., Castro-Díez, Y.: A 500-year precipitation record in Southern Spain. Int. J. Climatol.: J. R. Meteorol. Soc. **19**(11), 1233–1253 (1999)
3. Ramos-Calzado, P., Gómez-Camacho, J., Pérez-Bernal, F., Pita-López, M.F.: A novel approach to precipitation series completion in climatological datasets: application to Andalusia. Int. J. Climatol. **28**(11), 1525–1534 (2008)
4. Rodrigo, F.S., Gómez-Navarro, J.J., Montávez-Gómez, J.P.: Climate variability in Andalusia (southern Spain) during the period 1701–1850 based on documentary sources: evaluation and comparison with climate model simulations. Clim. Past **8**(1), 117–133 (2012)
5. Fernández-Montes, S., Rodrigo, F.S.: Trends in surface air temperatures, precipitation and combined indices in the southeastern Iberian Peninsula (1970–2007). Climate Res. **63**(1), 43–60 (2015)
6. Rodrigo, F.S., Esteban-Parra, M.J., Pozo-Vázquez, D., Castro-Díez, Y.: Rainfall variability in southern Spain on decadal to centennial time scales. Int. J. Climatol. **20**, 721–732 (2000)
7. Luque-Espinar, J.A., Chica-Olmo, M., Pardo-Igúzquiza, E., García-Soldado, M.J.: Influence of climatological cycles on hydraulic heads across a Spanish aquifer. J. Hydrol. **354**(1–4), 33–52 (2008)
8. Lomb, N.R.: Least-squares frequency analysis of unequally spaced data. Astrophys. Space Sci. **39**, 447–462 (1976)
9. Scargle, J.D.: Studies in astronomical time series analysis. II. Statistical aspects of spectral analysis of unevenly spaced data. Astrophys. J. **263**, 835–853 (1982)
10. Pardo-Igúzquiza, E., Rodríguez-Tovar, F.J.: Spectral and cross-spectral analysis of uneven time series with the smoothed Lomb-Scargle periodogram and Monte Carlo evaluation of statistical significance. Comput. Geosci. **49**, 207–216 (2012)
11. Confederación Hidrográfica del Guadalquivir (CHG). www.chguadalquivir.es
12. State Meteorological Agency (AEMET). http://www.aemet.es
13. Rodríguez-Tovar, F.J.: Orbital climate cycles in the fossil record: from semidiurnal to million-year biotic responses. Annu. Rev. Earth Planet. Sci. **42**, 69–102 (2014)
14. Climate Prediction Center. National Weather Center. http://www.cpc.ncep.noaa.gov/products/precip/CWlink/pna/nao.shtml
15. Climatic Research Unit, University of East Anglia. https://crudata.uea.ac.uk/cru/data/moi/